

## Upconversion Nanoprobes for the Ratiometric Luminescent Sensing of Nitric Oxide

Ningning Wang, Xinyan Yu, Ke Zhang, Chad A. Mirkin, and Jishan Li

*J. Am. Chem. Soc.*, **Just Accepted Manuscript** • DOI: 10.1021/jacs.7b06059 • Publication Date (Web): 27 Aug 2017

Downloaded from <http://pubs.acs.org> on August 27, 2017

### Just Accepted

“Just Accepted” manuscripts have been peer-reviewed and accepted for publication. They are posted online prior to technical editing, formatting for publication and author proofing. The American Chemical Society provides “Just Accepted” as a free service to the research community to expedite the dissemination of scientific material as soon as possible after acceptance. “Just Accepted” manuscripts appear in full in PDF format accompanied by an HTML abstract. “Just Accepted” manuscripts have been fully peer reviewed, but should not be considered the official version of record. They are accessible to all readers and citable by the Digital Object Identifier (DOI®). “Just Accepted” is an optional service offered to authors. Therefore, the “Just Accepted” Web site may not include all articles that will be published in the journal. After a manuscript is technically edited and formatted, it will be removed from the “Just Accepted” Web site and published as an ASAP article. Note that technical editing may introduce minor changes to the manuscript text and/or graphics which could affect content, and all legal disclaimers and ethical guidelines that apply to the journal pertain. ACS cannot be held responsible for errors or consequences arising from the use of information contained in these “Just Accepted” manuscripts.

# Upconversion Nanoprobes for the Ratiometric Luminescent Sensing of Nitric Oxide

Ningning Wang,<sup>†</sup> Xinyan Yu,<sup>†</sup> Ke Zhang,<sup>\*,†,‡</sup> Chad A. Mirkin,<sup>\*,†,§</sup> and Jishan Li<sup>\*,†</sup>

<sup>†</sup>Institute of Chemical Biology and Nanomedicine, State Key Laboratory of Chemo/Biosensing and Chemometrics, College of Chemistry and Chemical Engineering, Hunan University, Changsha, 410082, China.

<sup>‡</sup>Department of Chemistry and Chemical Biology, Northeastern University, 360 Huntington Ave, Boston, Massachusetts 02115, USA

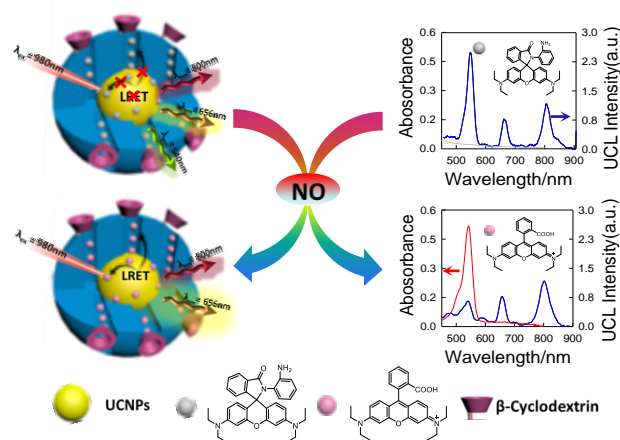
<sup>§</sup>Department of Chemistry and International Institute for Nanotechnology, Northwestern University, 2145 Sheridan Road, Evanston, Illinois 60208, USA

Supporting Information Placeholder

**ABSTRACT:** By taking advantage of the optical properties of upconversion nanoparticles (UCNPs), we have designed a luminescence ratiometric nanosensor for measuring nitric oxide (NO) in biological fluids, live cells, and tissues. This nanoconjugate consists of a UCNP core with two strong fluorescence emission peaks at 540 and 656 nm as the upconversion fluorophore, NO-reactive rhodamine B-derived molecules (RdMs) encapsulated within the mesopores of the mSiO<sub>2</sub> shell, and a  $\beta$ -cyclodextrin ( $\beta$ CD) layer on the exterior of the particle. Reaction of the analyte with the *O*-phenylenediamine of the RdM induces opening of the spiro-ring and is accompanied by an appearance of a strong rhodamine B (RdB) absorption band between 500~600 nm, which has spectral overlap with the green emission (540 nm) of the UCNPs. This results in an increase in the  $I_{656}/I_{540}$  ratio and quantitatively correlates with [NO]. The assay is validated under clean buffer conditions as well as in serum and liver tissue slices obtained from mouse models.

Nitric oxide (NO), which is produced by inducible and constitutive nitric oxide synthases (iNOS and cNOS), plays important roles in several biological processes, including those associated with immunological, cardiovascular, and nervous systems.<sup>1-3</sup> It is also implicated in the processes that protect against reactive oxygen-species.<sup>4</sup> Recently, studies have suggested that the reduction of NO is a major mechanism of hepatic ischemic-reperfusion injury (HIRI),<sup>5</sup> a condition that often arises intraoperatively from temporary inflow and/or outflow occlusions by vascular clamping. HIRI may result in multiple organ failures and/or systemic inflammatory response syndrome after surgery.<sup>6</sup> Therefore, monitoring the pharmacological parameters of HIRI in real time is critically important. Increased NO availability through the use of an NO precursor or donor has been associated with a reduction in the severity of HIRI.<sup>7</sup> Therefore, accurate measurement of NO levels in the blood or liver tissues in real time can provide a correlation with the progress

**Scheme 1. Schematic illustration of the sensing principle of the upconversion nanoprobe for ratiometric luminescent measurement of nitric oxide.**



of HIRI and help elucidate mechanisms through which anti-HIRI drugs function. While a range of organic fluorescent probes<sup>8</sup> and fluorescent nanosensors<sup>9</sup> have been developed to detect NO, the use of fluorescent probes in biological samples can sometimes be limited by the fluorophores' sensitivity to their environment, e.g. pH and hydrophobicity. In addition, fluorophore-based approaches are often hindered by high autofluorescence backgrounds of the complex biological fluids, poor membrane-penetration capability, and photo-bleaching. In contrast, lanthanide-doped upconversion nanoparticles (UCNPs) bypass many of these limitations. UCNPs are a unique class of luminescent probes that can convert continuous-wave (CW) near-infrared excitation to visible emission with a large anti-Stokes shift of several hundred nanometers, narrow emission bandwidths, and high resistance to photobleaching, which make them attractive for bioassays and deep-tissue imaging.<sup>10</sup> Herein, we have designed a novel UCNP-based upconversion ratiometric luminescence nanosensor to monitor NO in real time, and used these probes to study the protective activity of an anti-HIRI oligopeptide.

As shown in Scheme 1, the nanosensor consists

of a UCNP core with two strong luminescence emission peaks at 540 and 656 nm as the upconversion lumiphores. The core is surrounded by a shell of mesoporous SiO<sub>2</sub> (mSiO<sub>2</sub>), with pores loaded with rhodamine B-derived molecules (RdMs) (See SI: *Preparation of the Upconversion Nanoconjugate*). NO sensing is achieved by the luminescence resonance energy transfer (LRET) process between the RdMs and the UCNP. The shell is further modified with a layer of  $\beta$ -cyclodextrin ( $\beta$ CD) surface ligands to improve the nanoconjugate's stability and biocompatibility in physiological environments, and to block large molecules such as enzymes from entering the mesoporous channels while still allowing NO to penetrate freely. Reaction of NO with the *O*-phenylenediamine of RdM induces the opening of the spiro-ring<sup>8f</sup> and is accompanied by the recovery of the strong absorption of rhodamine B (RdB) at 500~600 nm, which spectrally overlaps with the green emission (540 nm) of UCNPs. Thus, the presence of NO increases the  $I_{656}/I_{540}$  ratio, allowing for the quantitative measurement of NO.

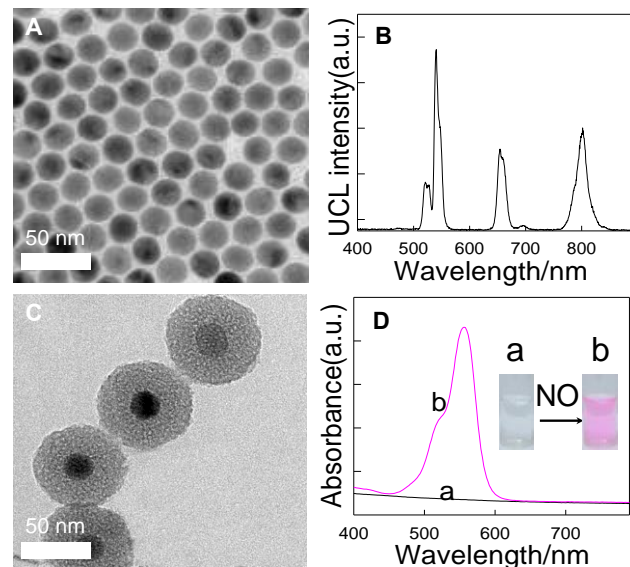


Figure 1. TEM image (A) and luminescence spectrum of UCNPs in cyclohexane (B),  $\lambda_{\text{exc}} = 980$  nm. (C) TEM image of UCNP@RdMMSN@ $\beta$ CD nanoconjugate. (D) UV/Vis spectra and visual appearance (inset) of the nanoconjugate ( $300 \mu\text{g}\cdot\text{mL}^{-1}$ ) before (a) and after (b) introduction of NO in PBS.

Transmission electron microscopy (TEM) shows that the oleic acid-capped UCNPs (NaYF<sub>4</sub>: 20% Yb, 2% Er, 0.2% Tm) have a uniform size of ~25 nm (Figure 1A). Luminescence spectroscopy gives three strong upconversion emission peaks at 540, 656 and 800 nm (Figure 1B), due to the doping of Er<sup>3+</sup> and Tm<sup>3+</sup> ions. The UCNP@RdMMSN@ $\beta$ CD particles have a ~20 nm thick mesoporous silica shell (Figure 1C), and possess excellent water dispersibility. Zeta-potential of the nanoconjugate is determined to be +22.7 mV, similar to that of the UCNP@MSN nanoparticles

(+23.7 mV), and significantly negative-shifted compared with that of the amine-terminated UCNP@MSN nanoparticles (+42.1 mV) (Figure S1). FTIR spectra show absorbance peaks at 3344 cm<sup>-1</sup> and 1636 cm<sup>-1</sup>, corresponding to the asymmetric and symmetric vibration modes of the OH groups (Figure S2). These two vibrations are much stronger for UCNP@RdMMSN@ $\beta$ CD nanoconjugates compared with the amine-modified UCNP@MSN particles. Therefore, both zeta-potential and FTIR analyses indicate that the  $\beta$ CD layer is successfully immobilized on the surface of the UCNP@MSN. To confirm the encapsulation of RdMs, the UV/Vis absorption spectra of the UCNP@RdMMSN@ $\beta$ CD nanoconjugates were taken before/after the addition of NO. It can be seen from Figure 1D that the absorption band at 500~600 nm of RdB appears when NO is present, and the solution color also changes from colorless to pink (inset of Figure 1D). FTIR shows strong absorbance peaks at 1384 cm<sup>-1</sup>, which is assigned to the stretching vibration of the C-O bond of -COO- groups after treatment with NO (Figure S3). These results indicate that RdMs are successfully coupled to UCNPs, and that the nanosensors are responsive to NO. By using an excess of NO to fully convert RdM to RdB and subsequently measuring RdB absorption, it is estimated that the loading efficiency of RdM is ~11.3 wt% (Figure S4).

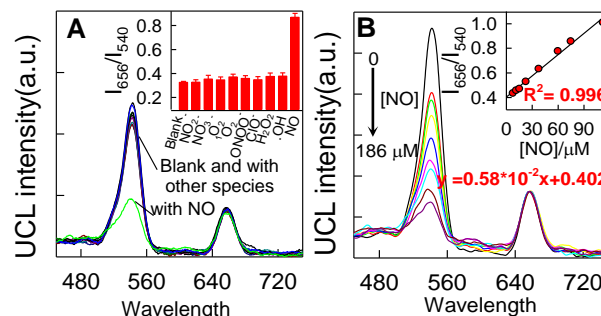


Figure 2. (A) UCL spectra and the luminescence intensity ratios of UCNP@RdMMSN@ $\beta$ CD ( $300 \mu\text{g}\cdot\text{mL}^{-1}$ ) in the presence of various chemical species (inset: chemical species tested; values are calculated from the spectra, 100  $\mu\text{M}$  for ROS and RNS, 75  $\mu\text{M}$  for NO). (B) Particle ( $300 \mu\text{g}\cdot\text{mL}^{-1}$ ) response to [NO] (0-186  $\mu\text{M}$ ) in PBS (10 mM, pH 7.4) at room temperature. Error bars are obtained from three parallel samples.  $\lambda_{\text{exc}}=980$  nm.

Next, we examined the solution stability and cytotoxicity of the upconversion nanoprobe. A RdB-leaching test with/without  $\beta$ CD modification was first performed. Because particles and their suspension media can be separated via centrifugation, and leached RdB would remain in the supernatant, leaching of RdB can be easily monitored. Figure S5 depicts the fluorescence intensities of the supernatants of the suspensions of the two nanoconjugates as a function of immersion time. The fluorescence intensity for the

UCNP@RdBMSN@ $\beta$ CD sample exhibits insignificant variations even after prolonged immersion times, while large increases of fluorescence can be observed for the non-capped sample, suggesting that  $\beta$ CD capping is effective in preventing RdB from leaching. In addition, the nanosensor  $I_{656}/I_{540}$  ratio remains stable in cell lysates for 24 h (Figure S6). An MTT cytotoxicity assay shows no evidence of cytotoxic for liver and HeLa cells up to 1 mg/mL for nanoprobe with or without prior with NO treatment (Figure S7), although the particles exhibit good cellular uptake (Figure S8). Z-scanning shows bright luminescence throughout the cells (Figure S9), and lysosomal staining (Figure S10) shows that the UCNP@MSN@ $\beta$ CD nanoconjugates colocalize with the lysosomes. These data suggest that the  $\beta$ CD-functionalized nanoconjugate has good stability and excellent cell permeability yet remains non-toxic to cells.

We next investigated the extent to which the luminescence intensity ratio ( $I_{656}/I_{540}$ ) changes when UCNP@RdMMSN@ $\beta$ CD particles are treated with NO and other reactive oxygen and nitrogen species under clean buffer conditions (Figure 2). With the addition of NO, upconversion luminescence (UCL) emission at 540 nm decreases, likely due to energy transfer from the UCNP to RdMs. In contrast, no obvious change is detected with other oxidative chemical species ( $\text{NO}_3^-$ ,  $\text{NO}_2^-$ ,  $\text{H}_2\text{O}_2$ ,  $\text{HClO}$ ,  $^1\text{O}_2$ ,  $\text{ONOO}^-$ ,  $\text{O}_2^-$  and  $\cdot\text{OH}$ ). These observations are similar to that of free RdMs (Figure S11). A plot of  $I_{656}/I_{540}$  ratio versus NO concentration in the range of 7.4–110  $\mu\text{M}$  reveals a linear response ( $R^2 = 0.996$ ), from which a detection limit of 73 nM based on a signal-to-noise ratio of  $S/N = 3$  is estimated. This range is appropriate for measuring NO in live cells ( $\sim 20 \mu\text{M}$ ),<sup>11</sup> serum ( $\sim 30\text{--}50 \mu\text{M}$ ),<sup>12</sup> or liver tis-

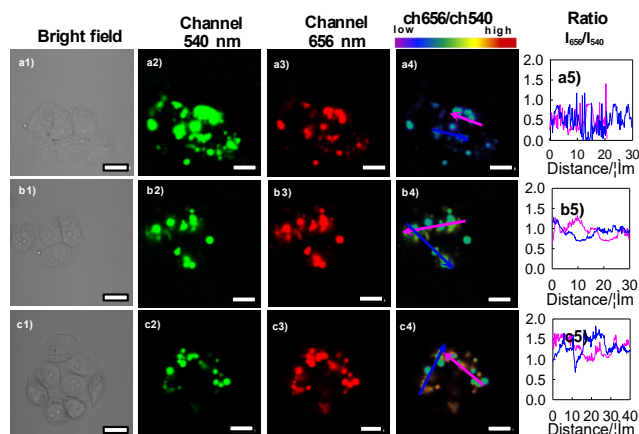


Figure 3. Confocal microscopy luminescence images of HeLa cells after treatment with UCNP@RdMMSN@ $\beta$ CD ( $300 \mu\text{g}\cdot\text{mL}^{-1}$ ) and different concentrations of NO (via DEA NONOate). Excitation: 980 nm. Scale bars: 25  $\mu\text{m}$ . a-c): No NO precursor, 0.2 mM and 0.4 mM, respectively; a4-c4): Luminescence ratiometric images displayed in pseudocolor. a5-c5): Intensity profiles of linear regions of across the HeLa cells shown in a4-c4.

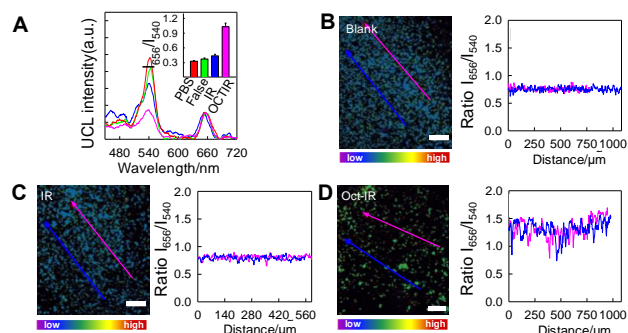


Figure 4. (A) UCL spectra and the luminescence intensity ratios (inset) of the nanoprobe in serum. Error bars were obtained from three parallel samples. (B–D) Luminescence ratiometric images at a depth of 300  $\mu\text{m}$  of rat liver tissue slices incubated with the nanoprobe ( $300 \mu\text{g}\cdot\text{mL}^{-1}$ ), and the corresponding intensity profile of a linear region across the liver tissue slices. Excitation: 980 nm. Scale bar: 200  $\mu\text{m}$ .

sues ( $\sim 40 \mu\text{M}$ ).<sup>13</sup>

To investigate the applicability of these probes for monitoring NO levels in live cells, we first incubated HeLa cells with the nanoprobe in cell growth medium. Then, the cells were treated with different amounts of NO, after which luminescence emission images at 540 and 656 nm were acquired (excitation: 980 nm). Under these artificially [NO]-elevated conditions, the luminescence emission for the 540 nm channel decreased with increasing [NO] (Figure 3). To demonstrate the possibility of using these probes to image NO in deep tissue (made possible by near-IR excitation), rat liver tissue slices (1–2 mm thick) were incubated with the nanoprobe and subsequently NO, and luminescence imaging was carried out using a confocal microscope equipped with a 980-nm laser. The Z-scans show clear upconversion luminescence emission at 656 nm even at a depth of 600  $\mu\text{m}$ , while the upconversion luminescence emission at 540 nm from the NO-treated tissue slice is substantially weaker (Figure S12).

Next, we used these NO-sensing probes to investigate the anti-HIRI behavior of octreotide (Oct), which is a synthetic somatostatin octapeptide that primarily inhibits the secretion of growth hormone.<sup>14</sup> Recent studies<sup>15</sup> have demonstrated that Oct can reduce HIRI significantly, possibly via elevation of NO concentrations, although a detailed mechanism remains unclear. Hepatic ischemia reperfusion surgery was performed on rat models with/without octreotide (Oct) pretreatment, and NO levels in the serum and liver tissue samples were monitored. As shown in Figure 4A, compared with blank (PBS), the green UCL emission at 540 nm decreases slightly for the serum of sham-operated rats and ischemia (IR) rat models, while the decrease was more substantial for the serum of the Oct-preconditioned IR (Oct-IR) rat model, resulting in

the corresponding luminescence intensity ratio ( $I_{656}/I_{540}$ ) changes. This suggests that there is only a small increase of serum NO level from sham to IR models (from  $\sim 16 \mu\text{M}$  to  $\sim 24 \mu\text{M}$ ), likely a result of self-protective stress responses, while the significant increase of NO levels for the Oct-IR group ( $\sim 86 \mu\text{M}$ ) corresponds with the activity of the drug. Confocal microscopy was also used to monitor the NO levels in living liver tissue slices obtained from the sham, IR, and Oct-IR rat groups after incubation with the up-conversion nanoprobe (Figure 4B-D). The luminescence emission ratio of  $I_{656}/I_{540}$  increased significantly for the Oct-IR model, while no clear difference was found for the sham and the IR models, indicating that Oct is linked to elevated NO levels in the liver tissue. This points to the possibility that the protective mechanisms of Oct on HIRI are at least in part due to increased NO production.

In summary, we have developed a novel upconversion ratiometric nanosensor for NO monitoring, which takes advantage of the excellent optical characteristics of UCNPs, the highly selective RdMs/NO ring-opening reaction, and the biocompatibility and size filtering properties of  $\beta\text{CD}$ . Using this novel probe, we discovered that NO levels are elevated in Oct-treated rat IR models. To the best of our knowledge, this is the first time that an upconversion luminescent nanoprobe has been successfully used to measure serum and liver tissue NO levels in HIRI and to study the drug-protection process. With further optimization, this new NO-sensing platform could become a highly useful biotechnology tool for *in vitro* and *in vivo* monitoring of NO, and may be extended to additional analytes.

## ASSOCIATED CONTENT

### Supporting Information.

Experimental details and other additional information as noted in text. This material is available free of charge via the Internet at <http://pubs.acs.org>.

## AUTHOR INFORMATION

### Corresponding Author

\*jishanli@hnu.edu.cn

\*k.zhang@northeastern.edu

\*chadnano@northwestern.edu

### ORCID

Jishan Li:0000-0001-8144-361X

### Notes

The authors declare no competing financial interest.

## ACKNOWLEDGMENT

This work was supported by NSFC (21475036, 21527810), and the Hunan Provincial Natural Science Foundation (2016JJ1005).

## REFERENCES

- [1] Ignarro, L. J. *Nitric Oxide Biology and Pathobiology*. Academic Press: San Diego, **2000**.
- [2] Garthwaite, J. E. J. *Neurosci.* **2008**, *27*, 2783-2802.
- [3] Pluth, M. D.; Tomat, E.; Lippard, S. J. *Annu. Rev. Biochem.* **2011**, *80*, 333-355.
- [4] Darley-Usmar, V.; Wiseman, H.; Halliwell, B. *FEBS Letters*. **1995**, *369*, 131-135.
- [5] (a) Hsu, C.-M.; Wang, J.-S.; Liu, C.-H.; Chen, L.-W. *Shock*. **2002**, *17*, 280-285. (b) Koti, R. S.; Seifalian, A. M.; Davidson, B. R. *Dig. Surg.* **2003**, *20*, 383-396. (c) bu-Amara, M.; Yang, S. Y.; Quaglia, A.; Rowley, P.; de Mel, A.; Tapuria, N.; Seifalian, A.; Davidson, B.; Fuller, B. *Clin Sci (Lond)*. **2011**, *121*, 257-266.
- [6] Teoh, N. C.; Farrell, G. C. J. *Gastroen. Hepatol.* **2003**, *18*, 891-902.
- [7] (a) Kuroki, I.; Miyazaki, T.; Mizukami, I.; Matsumoto, N.; Matsumoto, I. *Hepatogastroenterology*. **2004**, *51*, 1404-1407. (b) Kurabayashi, M.; Takeyoshi, I.; Yoshinari, D.; Koibuchi, Y.; Ohki, T.; Matsumoto, K.; Morishita, Y. *J. Invest. Surg.* **2005**, *18*, 193-200. (c) Elrod, J. W.; Duranski, M. R.; Langston, W.; Greer, J. J. M.; Tao, L.; Dugas, T. R.; Kevil, C. G.; Champion, H. C.; Lefer, D. J. *Circ. Res.* **2006**, *99*, 78-85.
- [8] (a) Nagano, T.; Yoshimura, T. *Chem. Rev.* **2002**, *102*, 1235-1270. (b) Kobayashi, H.; Ogawa, M.; Alford, R.; Choyke, P. L.; Urano, Y. *Chem. Rev.* **2010**, *110*, 2620-2640. (c) Chen, X.; Tian, X.; Shin, I.; Yoon, J. *Chem. Soc. Rev.* **2011**, *40*, 4783. (d) Yu, H.; Xiao, Y.; Jin, L. *J. Am. Chem. Soc.* **2012**, *134*, 17486-17489. (e) Sun, Y. Q.; Liu, J.; Zhang, H.; Huo, Y.; Lv, X.; Shi, Y.; Guo, W. *J. Am. Chem. Soc.* **2014**, *136*, 12520-12523. (f) Chen, X.; Pradhan, T.; Wang, F.; Kim, J. S.; Yoon, J. *Chem. Rev.* **2012**, *112*, 1910-1956. (g) Chan, J.; Dodani, S. C.; Chang, C. J. *Nat Chem.* **2012**, *4*, 973-984. (h) Mao, Z.; Feng, W.; Li, Z.; Zeng, L.; Lv, W.; Liu, Z. *Chem. Sci.* **2016**, *7*, 5230-5235. (i) Lim, M. H.; Lippard, S. J. *Acc chem res.* **2007**, *40*, 41-51. (j) Apfel, U.-P.; Buccella, D.; Wilson, J. J.; Lippard, S. J. *Inorg Chem.* **2013**, *52*, 3285-3294.
- [9] (a) Kim, J.-H.; Heller, D. A.; Jin, H.; Barone, P. W.; Song, C.; Zhang, J.; Trudel, L. J.; Wogan, G. N.; Tannenbaum, S. R.; Strano, M. S. *Nat Chem.* **2009**, *1*, 473-481. (b) Wu, P.; Wang, J.; He, C.; Zhang, X.; Wang, Y.; Liu, T.; Duan, C. *Adv Funct Mater.* **2012**, *22*, 1698-1703. (c) Eroglu, E.; Gottschalk, B.; Charoensin, S.; Blass, S.; Bischof, H.; Rost, R.; Madreiter-Sokolowski, C. T.; Pelzmann, B.; Bernhart, E.; Sattler, W.; Hallström, S.; Malinski, T.; Waldeck-Weiermair, M.; Graier, W. F.; Malli, R. *Nat Commun.* **2016**, *7*, 10623-10633. (d) Li, Y.; Wu, W.; Yang, J.; Yuan, L.; Liu, C.; Zheng, J.; Yang, R. *Chem. Sci.* **2016**, *7*, 1920-1925.
- [10] (a) Wang, F.; Liu, X. *Chem. Soc. Rev.* **2009**, *38*, 976-989; (b) Bünzli, J.-C. G. *Chem. Rev.* **2010**, *110*, 2729-2755. (c) Zhou, J.; Liu, Z.; Li, F. *Chem. Soc. Rev.* **2012**, *41*, 1323-1349. (d) Hao, S.; Chen, G.; Yang, C. *Theranostics.* **2013**, *3*, 331-345. (e) Chen, G.; Qiu, H.; Prasad, P. N.; Chen, X. *Chem. Rev.* **2014**, *114*, 5161-5214. (f) Li, Z.; Liang, T.; Lv, S.; Zhong, Q.; Liu, Z. *J. Am. Chem. Soc.* **2015**, *137*, 11179-11185. (g) Peng, J.; Samanta, A.; Zeng, X.; Han, S.; Wang, L.; Su, D.; Loong, D. T. B.; Kang, N. Y.; Park, S. J.; All, A. H.; Jiang, W.; Yuan, L.; Liu, X.; Chang, Y. T. *Angew. Chem., Int. Ed.* **2017**, *56*, 4165-4169.
- [11] Li, M.; Wang, L.; Liu, H.; Su, B.; Liu, B.; Lin, W.; Li, Z.; Chang, L. *J. South. Med. Univ.* **2013**, *12*, 1752-1756.
- [12] (a) Lang, J.; Zhang, P. *Mil. Med. Sci.* **2014**, *10*, 814-818. (b) Miranda, K. M.; Espey, M. G.; Wink, D. A. *Nitric oxide.* **2001**, *5*, 62-71.
- [13] Li, Y.; Xu, X.; Ji, H.; Lei, T. *Chinese Hepatol.* **2002**, *1*, 20-21.
- [14] (a) Brazeau, P.; Vale, W.; Burgus, R.; Ling, N.; Butcher, M.; Rivier, J.; Guillemin, R. *Science.* **1973**, *179*, 77-79. (b) Burgus, R.; Ling, N.; Butcher, M.; Guillemin, R. *Proc. Natl. Acad. Sci. U.S.A.* **1973**, *70*, 684-688.
- [15] (a) Yang, J.; Sun, H.; Guan, R.; Liu, W.; Xia, Y.; Zhao, J.; Liu, J. *Transplant. Proc.* **2014**, pp 3282-3288. (b) Bloechle, C.; Kusterer, K.; Konrad, T.; Hosch, S.; Izbicki, J.; Knoefel, W.; Broelsch, C.; Usadel, K. *Horm. Metab. Res.* **1994**, *26*, 270-275.

TOC

